Proceedings of the 17th World Congress
The International Federation of Automatic Control
Seoul, Korea, July 6-11, 2008

GL_2 Estimation of Front Wheel Disturbance ⋆

Ahmad Akbari, **Boris Lohmann** and **Behnam Salimbahrami**

Institute of Automatic Control,
Technical University of Munich, Germany.
email: {akbari, lohmann, salimbahrami}@tum.de

Abstract: This paper concerns with the generalized L_2 estimation of the disturbance applied to a vehicle steer wheel. The study is specially useful for active vehicle suspensions utilizing wheelbase preview information. To design an estimator to perform satisfactorily for a wide range of road irregularities and to care for system structured (parametric) uncertainties, a generalized L_2 gain based scheme is proposed to design the estimator. The problem is formulated using LMI's and to ensure desired transient dynamics for the system, some pole location constraints are considered. To evaluate the effectiveness of the proposed controller it is compared with a Kalman estimator designed under similar conditions. The results demonstrate effectiveness of the proposed estimator.

1. INTRODUCTION AND MOTIVATION

A vehicle suspension system is responsible for ride comfort of passengers, without sacrificing ride safety, and other handling requirements. These requirements are highly conflicting. To cope with the indispensable trade-off between these requirements along with road profile, many active suspension approaches have been proposed, which have improved system performance to a considerable extent, see, e.g., (Hrovat, D. [1997]) and references therein. However, an interesting control scheme considered for active vehicle suspension design, is to include a feedforward term (or preview control) in feedback controller. This scheme involves the acquisition and use of information concerning the road profile ahead of vehicle to 'prepare' the system for oncoming disturbance (Hac, A. [1992]).

A preview-based suspension system lifts the wheel over the bump to reduce the forces transmitted to the body to provide more comfort for the passengers.
There are two ways to obtain preview information, one using a "look-ahead" sensor and the other by estimating road profile from the system response, referring to as wheelbase preview (Wu, L. and Chen, H.L. [2006]). Look-ahead preview systems, even though have been shown to lead to enhanced system performance compared to their pure feedback counterpart, they suffer the drawback of wrong detection / interpretation of road irregularities when facing pseudo-obstacles, e.g., a paper stack or a hole filled with turbulent rainwater. These situations may not only lose vehicle road holding and hence its stability, but also its steering cannot be accomplished as desired. Clearly, a vehicle with slippery front (steer) wheels is no longer controllable and independently from steering angle travels straight-ahead, and with slippery rear (drive) wheels is even unstable (Foag, W. [1990]).

From this point of view wheelbase preview is more promising. Moreover, it imposes no additional costs for the sensor. This scheme has already been studied in some papers, e.g., (Marzbanrad, J., Ahmadi, G., Zohoor, H. and Hojjat, Y. [2004]). but they assume that road data of the front wheel is available. Therefore, the objective of this paper is to fill the gap between and obtain a robust estimation of the road disturbance applied to the front wheel from system response.

To care for the wide range of road irregularities, a generalized L_2 (GL_2)-gain based scheme is used to design the estimator. Noting that system uncertainties are parametric (structured), this schem leads to a less conservative design than H_∞. Moreover, to ensure desired transient dynamics for the system, some pole location constraints are considered. It is also worthwhile to mention that the design scheme allows the designer to emphasize on specific states to get more accurate estimation of road disturbance. Frequency-dependent weights lead to more accurate disturbance detection on specific frequency range.

This study is also useful for adaptive (gain scheduled) active suspensions where the road type is the scheduling variable. In addition, noting that the approach is based on state estimation, it can also be utilized in state feedback suspensions.

The half car model used in this study is described in section II, Section II also describes the problem and gives the framework for the design. section III gives the LMI-based solution for problem. This section is followed by the design of above mentioned estimator. In addition, in this section for the sake of comparison, a Kalman estimator is also designed. In section IV some numerical simulation is carried out to compare both estimators and section V contains concluding remarks.

2. SYSTEM DESCRIPTION AND PROBLEM FORMULATION

A pitch-plane (bicycle) half-car model, as shown in Figure 1, is used in this study. It consists of the sprung (body) mass, two unsprung masses(wheel-axle assemblies) and the suspension system placed between them. The suspension system in this study, without loss of generality, is assumed to be passive, i.e., it comprises a spring parallel to a damper. The nomenclature used and parameter values are given in Table I. Note that the body mass changes with the vehicle load and here it is assumed that it has a variation of 30% around its nominal value and can be measured online.

The sprung mass is assumed to be rigid and has freedom of motion in heave and pitch directions. Either of unsprung masses

⋆ This work is partially supported by the Sahand University of Technology, MSRT, Iran.

Model parameters (symbols)	values
sprung mass (m_s)	$730 \pm 30\%$ kg
pitch moment of inertia (I)	1230 $kg.m^2$
distance between C.G. and front axle (l_f)	1.011 m
distance between C.G. and rear axle (l_r)	1.803 m
front suspension stiffness (k_{sf})	19960 N/m
rear suspension stiffness (k_{sr})	17500 N/m
front suspension damping rate (b_{sf})	1290 N/(m/sec)
rear suspension damping rate (b_{rf})	1620 N/(m/sec)
front unsprung mass (m_{uf})	40 kg
rear unsprung mass (m_{ur})	35.5 kg
front tire stiffness (k_{tf})	175500 N/m
rear tire stiffness (k_{tr})	175500 N/m
road roughness coefficient (G_0)	5.12×10^{-6} m
vehicle forward velocity (V)	20 m/s

Table 1. Nomenclature and values of the parameters in a half car model

has the freedom of motion in vertical direction. Thus the half car model has four degrees of freedom.

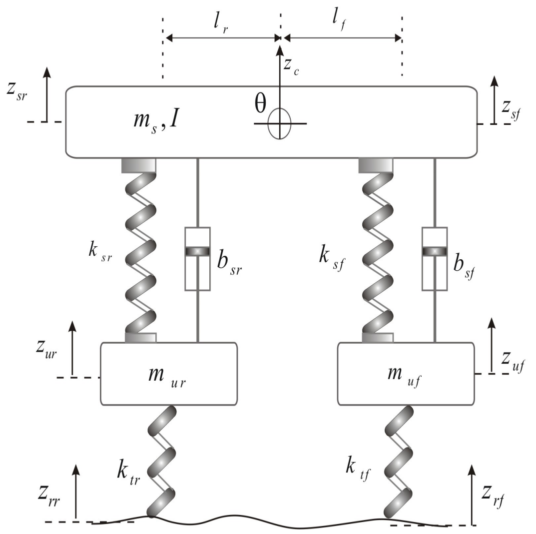

Fig. 1. suspension system

According to the variables defined on the figure and assuming that the pitch motion is small enough, the equations governing the motions of sprung and unsprung masses are given by:

$$\begin{aligned} &m_s\ddot{z}_c = f_f + f_r, \\ &I\ddot{\theta} = f_f l_f - f_r l_r, \\ &m_{uf}\ddot{z}_{uf} = -k_{tf}(z_{uf} - z_{rf}) - f_f, \\ &m_{ur}\ddot{z}_{ur} = -k_{tr}(z_{ur} - z_{rr}) - f_r, \end{aligned} \tag{1}$$

Where

$$\begin{aligned} f_f &= u_f - k_{sf}(z_c + l_f\theta - z_{uf}) - b_{sf}(\dot{z}_c + l_f\dot{\theta} - \dot{z}_{uf}), \\ f_r &= u_r - k_{sr}(z_c - l_r\theta - z_{ur}) - b_{sr}(\dot{z}_c - l_r\dot{\theta} - \dot{z}_{ur}) \end{aligned}$$

The uncertain parameter m_s, which occurs in the denominator of the differential equation, can be represented by the following linear fractional transformation (Zhou, K., Doyle, J. and Glover, K. [1996]):

$$\frac{1}{m_s} = \frac{1}{\bar{m}_s(1 + d\delta)} = \mathcal{F}_l\left(\begin{pmatrix} \frac{1}{\bar{m}_s} & -\frac{1}{\bar{m}_s} \\ 1 & -d \end{pmatrix}, \delta\right)$$

where $|\delta| < 1$ and d represents the variation percentage around the nominal value. Now, following the approach of (Zhou, K., Doyle, J. and Glover, K. [1996], Gaspar, P. and Bokor, J. [2003]), after some manipulation, differential equations of the system are obtained as:

$$\begin{aligned} &M_s\ddot{q} = GB_s(\dot{z}_u - \dot{z}_s) + GK_s(z_u - z_s) + F\nu, \\ &M_u\ddot{z}_u = B_s(\dot{z}_s - \dot{z}_u) + K_s(z_s - z_u) + K_t(z_r - z_u), \\ &\epsilon = (1\ 1)\{B_s(\dot{z}_s - \dot{z}_u) + K_s(z_s - z_u)\} - d\nu \end{aligned} \tag{2}$$

where $\nu = \delta\epsilon$ represents the uncertainty and

$$q = \begin{pmatrix} z_c \\ \theta \end{pmatrix},\ z_s = \begin{pmatrix} z_{sf} \\ z_{sr} \end{pmatrix},\ z_u = \begin{pmatrix} z_{uf} \\ z_{ur} \end{pmatrix},\ z_r = \begin{pmatrix} z_{rf} \\ z_{rr} \end{pmatrix}$$

and the matrices of sprung mass (M_s), unsprung mass (M_u), suspension stiffness (K_s), suspension damping (B_s), tire stiffness (K_t), geometry (G) and F, are given as:

$$\begin{aligned} M_s &= \begin{pmatrix} m_s & 0 \\ 0 & I_\theta \end{pmatrix},\ M_u = \begin{pmatrix} m_{uf} & 0 \\ 0 & m_{ur} \end{pmatrix}, \\ K_s &= \begin{pmatrix} k_{sf} & 0 \\ 0 & k_{sr} \end{pmatrix},\quad B_s = \begin{pmatrix} b_{sf} & 0 \\ 0 & b_{sr} \end{pmatrix}, \\ K_t &= \begin{pmatrix} k_{tf} & 0 \\ 0 & k_{tr} \end{pmatrix},\quad G = \begin{pmatrix} 1 & 1 \\ l_f & -l_r \end{pmatrix}, \\ F^T &= (-d\ 0), \end{aligned}$$

Assuming that the pitch motion is small enough, the following linear approximations can be applied

$$z_{sf} = z_c + l_f\theta,$$
$$z_{sr} = z_c - l_f\theta$$

which yields

$$z_s = G^T q$$

therefore, left-multiplying $G^T M_s^{-1}$ both sides of the first equation in 2, we arrive at:

$$\ddot{z}_s = N[B_s(\dot{z}_u - \dot{z}_s) + K_s(z_u - z_s)] + L^T M_s^{-1} F\nu$$

where $N := G^T M_s^{-1} G$. Choosing the set of state variables as:

$$x^T = \left((z_s - z_u)^T\ \dot{z}_s^T\ (z_u - z_r)^T\ \dot{z}_u^T\right) \in \mathbb{R}^8$$

and $w = (w_f\ w_r)^T = \dot{z}_r$ (ground vertical velocity) as disturbance input, the state space description of the system is obtained as:

$$\begin{aligned} &\dot{x}(t) = Ax + B_\nu\nu + B_w w, \\ &\epsilon = C_\epsilon x - d\nu, \end{aligned}$$

where

$$\begin{aligned} A &= \begin{pmatrix} 0 & I & 0 & -I \\ -NK_s & -NB_s & 0 & NB_s \\ 0 & 0 & 0 & I \\ M_u^{-1}K_s & M_u^{-1}B_s & -M_u^{-1}K_t & -M_u^{-1}B_s \end{pmatrix}, \\ B_\nu &= \begin{pmatrix} 0 \\ L^T M_s^{-1} F \\ 0 \\ 0 \end{pmatrix}, B_w = \begin{pmatrix} 0 \\ 0 \\ -I \\ 0 \end{pmatrix} \\ C_\epsilon &= (1\ 1)(-K_s\ -B_s\ 0\ B_s) \end{aligned}$$

The goal of this paper is to estimate the road disturbance applied to the steer wheel (w_f) from system response. The estimator design framework is depicted in Figure 2 .

It is assumed that suspension deflections ($z_s - z_u$) and vertical accelerations of the sprung mass ($\ddot{z}_s$) are the measured outputs

(y). These outputs can be readily measured in practice using suitable displacement sensors and accelerometers respectively. The performance output of z, noting the relation

$$w_f = \dot{z}_{rf} = \dot{z}_{uf} - \dot{x}_5 = x_7 - \dot{x}_5$$

is assumed to comprise only these relevant states, i.e., x_5 and x_7. Clearly the more precise estimation of these states, the more accurate detected road disturbance.

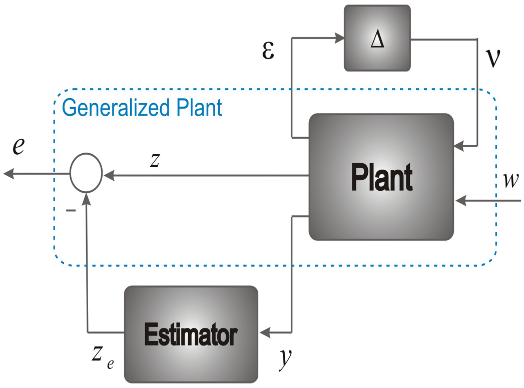

Fig. 2. Estimator design framework

3. ESTIMATOR DESIGN

3.1 Design scheme

This section gives a brief overview of estimator design approach employed in this study. For a generality, let the generalized plant $P(s)$ of Figure 2 is described by the following state-space realization:

$$\begin{aligned} \dot{x}(t) &= Ax + B_\nu \nu + B_w w, \\ \epsilon &= C_\epsilon x + D_{\epsilon\nu}\nu + D_{\epsilon w} w, \\ e &= C_z x + D_{z\nu}\nu + D_{zw} w - z_e, \\ y &= C_y x + D_{y\nu}\nu + D_{yw} w \end{aligned} \tag{3}$$

where $x(t) \in \mathbb{R}^n$ is the state vector, $w(t) \in \mathbb{R}^m$ is exogenous input, $z(t) \in \mathbb{R}^p$ is the performance output vector, $y(t) \in \mathbb{R}^{p_y}$ is the measured output vector and ϵ and ν represent the output and input vector corresponding to uncertainty block. Without any complication, the normalizing weighting functions of exogenous input and performance output can be embedded in the plant.

Now, as in Figure 2 interconnect the generalized plant of (3) with the dynamic estimator $F(s)$. The goal is to find an Estimator $F(s)$ such that $e = z - z_e$ is kept as small as possible, for all disturbances w and against system uncertainties.

To design an estimator to perform satisfactorily for a wide range of road irregularities, not just white noises, and to care for system structured (parametric) uncertainties, calls for employing generalized L_2 (GL_2) gain as a measure of estimation quality. The GL_2 design is a generalization of H_∞ design, which leads to a less conservative design when system uncertainties are structured (Wang, J. and Wilson, D. A. [2001], D'andrea, R. [1999]). Therefore, the objective is to find $F(s)$ such that the resulting system is internally stable, and the GL_2 gain of the system from $\bar{w} = \begin{pmatrix}\nu^T & w^T\end{pmatrix}^T$ to $\bar{e} = \begin{pmatrix}\epsilon^T & e^T\end{pmatrix}^T$ is smaller than γ, a specified positive number, i.e.,

$$\|T\|_{GL_2} = \left\| \frac{\bar{e}}{\bar{w}} \right\|_{GL_2} < \gamma \tag{4}$$

Henceforth, we consider the following description for the generalized plant:

$$\begin{aligned} \dot{x}(t) &= Ax + B_1\bar{w}, \\ \bar{e} &= C_1 x + D_{11}\bar{w} + D_{12} z_e, \\ y &= C_2 x + D_{21}\bar{w} \end{aligned} \tag{5}$$

Let the estimator $F(s)$ to be designed is represented in state space form by:

$$\begin{aligned} \dot{x}_e(t) &= A_e x_e + B_e y, \\ z_e &= C_e x_e + D_e y \end{aligned}$$

Then the closed loop system has the following state space realization:

$$\begin{pmatrix} \dot{\xi} \\ \bar{e} \end{pmatrix} = \left(\begin{array}{c|c} \mathcal{A} & \mathcal{B} \\ \hline \mathcal{C} & \mathcal{D} \end{array}\right) \begin{pmatrix} \xi \\ \bar{w} \end{pmatrix} \tag{6}$$

where $\xi = \begin{pmatrix} x \\ x_e \end{pmatrix}$ and closed loop state space matrices are obtained by:

$$\begin{aligned} \mathcal{A} &:= \begin{pmatrix} A & 0 \\ B_e C_2 & A_k \end{pmatrix}, \mathcal{B} := \begin{pmatrix} B_1 \\ B_e D_{21} \end{pmatrix} \\ \mathcal{C} &:= \begin{pmatrix} C_1 + D_{12} D_e C_2 & D_{12} C_e \end{pmatrix} \\ \mathcal{D} &:= D_{11} + D_{12} D_e D_{21} \end{aligned} \tag{7}$$

As in (Wang, J. and Wilson, D. A. [2001]), we consider the the sets $\mathcal{D}$ and $\mathcal{E}$, which define the allowable disturbance and cost criterion, as :

$$\begin{aligned} \mathcal{D} &:= \{d_k \in L_2 : \|d_k\| \leq 1, k \in [1, m] \subset \mathbb{Z}^+\}, \\ \mathcal{E} &:= \{e_l \in L_2 : \|e_l\| \leq 1, l \in [1, n] \subset \mathbb{Z}^+\} \end{aligned}$$

Note that the sets, unlike H_∞, are not restricted to be balls in L_2. Now based on the results of (Wang, J. and Wilson, D. A. [2001], D'andrea, R. [1999]), $\|T\|_{GL_2} < \gamma$ if and only if there exists a symmetric positive definite matrix

$$\mathcal{X} \succ 0 \tag{8a}$$

and

$$\begin{aligned} R &:= r_1 I_{d_1} \oplus r_2 I_{d_2} \oplus \cdots \oplus r_m I_{d_m} > 0, \\ S &:= s_1 I_{e_1} \oplus s_2 I_{e_2} \oplus \cdots \oplus s_n I_{e_m} > 0 \end{aligned}$$

with

$$r_k, s_l \in \mathbb{R}^+ \text{ and } \sum_{k=1}^{m} r_k < \gamma, \ \sum_{l=1}^{n} s_l < \gamma$$

such that:

$$\begin{pmatrix} \mathcal{A}^T\mathcal{X} + \mathcal{X}\mathcal{A} & * & * \\ \mathcal{B}^T\mathcal{X} & -R & * \\ \mathcal{C} & \mathcal{D} & -S \end{pmatrix} \prec 0 \tag{8b}$$

where $*$ represents the transpose of the elements across the diagonal. It is clear that setting R and S to γI, reduces the problem to an H_∞ one (Boyd, S., Ghaoui, L.E., Feron, E. and Balakishnan, V. [1994]).

In addition, in order to guarantee desired transient dynamics for the system, some pole placement constraints are imposed. Here we consider the desired pole location as the combination of the following pole constraints:

(1) Disk region ($|s| < \rho$), which can prevent fast estimator dynamics and therefore makes it easier to implement using digital computers. All eigenvalues of $\mathcal{A}$ lie in a disk with radius ρ centered at the origin if and only if there exists a matrix $\mathcal{X}$ satisfying (Chilali, M. and Pascal, G. [1996])

$$\begin{pmatrix} -\rho\mathcal{X} & \mathcal{X}\mathcal{A} \\ * & -\rho\mathcal{X} \end{pmatrix} \prec 0 \tag{8c}$$

Note that as usual in multi-objective design framework (Scherer, C.W., Gahinet, P. and Chilali, M. [1997]), we have used the same decision matrix $\mathcal{X}$ of GL_2 for the above constraint.

(2) α-stability region ($Re(s) < -\alpha$), which ensures a minimum damping coefficient of α and is represented by the following LMI:

$$\mathcal{A}^T\mathcal{X} + \mathcal{X}\mathcal{A} + 2\alpha\mathcal{X} \prec 0 \tag{8d}$$

substitution of calligraphic matrices in the LMI's (8) with their values of (7), they lead to bilinear matrix inequalities, which can not be solved by numerically tractable methods. To manage the problem, we apply the linearizing idea of (Chilali, M. and Pascal, G. [1996], Scherer, C.W., Gahinet, P. and Chilali, M. [1997]). To this goal, partition $\mathcal{X}$ and $\mathcal{X}^{-1}$ as:

$$\mathcal{X} = \begin{pmatrix} X & M \\ M^T & \star \end{pmatrix}, \mathcal{X}^{-1} = \begin{pmatrix} Y & N \\ N^T & \star \end{pmatrix}$$

where $\star$ represents that the block is arbitrary. X and Y are symmetric and of the same size as A. Also define:

$$\mathcal{Y} = \begin{pmatrix} I & Y \\ 0 & N^T \end{pmatrix}$$

Let us now define the change of estimator variables as follows:

$$\begin{aligned} \hat{A} &:= YAX + NB_eC_2X + NA_kM^T, \\ \hat{B} &:= NB_e, \\ \hat{C} &:= D_eC_2X + C_eM^T, \\ \hat{D} &:= D_e \end{aligned} \tag{9}$$

If we perform congruence transformations with $\mathcal{Y}$, $diag(\mathcal{Y}, I, I)$, $diag(\mathcal{Y}, \mathcal{Y})$ and $\mathcal{Y}$on the LMI's (8) respectively, we obtain:

$$\begin{pmatrix} X & I \\ I & Y \end{pmatrix} \succ 0 \tag{10a}$$

$$\begin{pmatrix} AX + XA^T & * & * & * \\ B_1 & -R & * & * \\ \hat{A} + A^T & YB_1 + \hat{B}D_{21} & A^TY + YA + \hat{B}C_2 + C_2^T\hat{B}^T & * \\ C_1X + D_{12}\hat{C} & D_{11} + D_{12}\hat{D}D_{21} & C_1 + D_{12}\hat{D}C_2 & -S \end{pmatrix} \prec 0 \tag{10b}$$

$$\begin{pmatrix} -\rho X & -\rho I & AX & A \\ -\rho I & -\rho Y & \hat{A} & YA + \hat{B}C_2 \\ * & * & -\rho X & -\rho I \\ * & * & -\rho I & -\rho Y \end{pmatrix} \prec 0 \tag{10c}$$

$$\begin{pmatrix} AX + XA^T + 2\alpha X & \hat{A} + A^T + 2\alpha I \\ * & A^TY + YA + \hat{B}C_2 + C_2^T\hat{B}^T + 2\alpha Y \end{pmatrix} \prec 0 \tag{10d}$$

Now we can formulate GL_2 estimator design by the following optimization problem in LMI's:

$$\min_{\gamma,X,Y,\hat{A},\hat{B},\hat{C},\hat{D},r_k,s_l,R,S} \gamma, \text{subject to LMI's}(10)$$

Given any solution of this LMI, compute via SVD a full-rank factorization $MN^T = I - XY$ (this equation is readily obtained form $\mathcal{X}\mathcal{X}^{-1} = I$) of the matrix $I - XY$ and then solve the system of linear equations (9) for D_e, C_e, B_e and A_e (in this order).

3.2 Application to the problem

Now the proposed approach is applied to design an GL_2 estimator for the problem described in section II. The problem has already been cast into desired design scheme. But noting the fact that human body is more sensitive to vertical body accelerations in the frequency range 4-8 HZ and to rotational accelerations in the 1-2 Hz, calls for more accurate estimation in this frequency range. The following weighting function is considered for the error ($e = z - z_e$) to emphasize on importance of minimization in this frequency range.

$$W_e = \frac{s^2 + 54s + 987}{s^2 + 37s + 987}$$

In the design process, for the pole placement constraints the following values are considered:

$$\alpha = 1, \rho = 150$$

By applying the procedure in the preceding subsection in Matlab environment (Gahinet, P., Nemirovski, A., Laub, A.J. and Chilali, M. [1995]), the GL_2 estimator was computed.

Remark 1. It is worth mentioning that some other parametric uncertainties (e.g., tire stiffness) can be considered in the system and then treated in similar way. It is shown in (D'andrea, R. [1999]) that GL_2 design for a full structured uncertainty can improve H_∞ performance up to $\sqrt{N}$ times, i.e.

$$\|T\|_\infty \le \|T\|_{GL_2} \le \sqrt{N}\|T\|_\infty$$

where N is the number of uncertainty blocks.

To demonstrate the effectiveness of the obtained estimator, also a Kalman estimator is designed to solve the problem under study. A fair comparison requires that the design of both estimators be accomplished under similar design requirements. Since in the design of the GL_2 estimator we ignored the measurement noise (clearly it can be readily included in the design without any complication), in the design of Kalman estimator, matrices Q (disturbance covariance) and R (measurement noise covariance) are assumed as I and $0.1 * I$ respectively, to represent the accuracy of measurements.

The designed estimators will be compared in the next section.

4. SIMULATION RESULTS

To evaluate the effectiveness of the proposed estimator, in the following some frequency and time domain simulations are carried out.

4.1 Frequency response

Figure 3 shows the closed loop frequency response from front ground vertical velocity $w_f = \dot{z}_{rf}$ to the estimation error e, using both Kalman and GL_2 estimators, under different values of sprung mass (m_s). It can be seen that GL_2 estimator in the frequency range of interest (1-8 Hz) provides a significant reduction in the magnitude. This is also true when sprung mass changes. (The sprung mass values considered for the simulation are: $0.75m_{s,n}$, $m_{s,n}$ and $1.25m_{s,n}$). These plots also reveal that the frequency response shape of GL_2 based system, compared to that of Kalman based, shows slight changes with the change of sprung mass, confirming that it possesses more robustness than Kalman estimator.

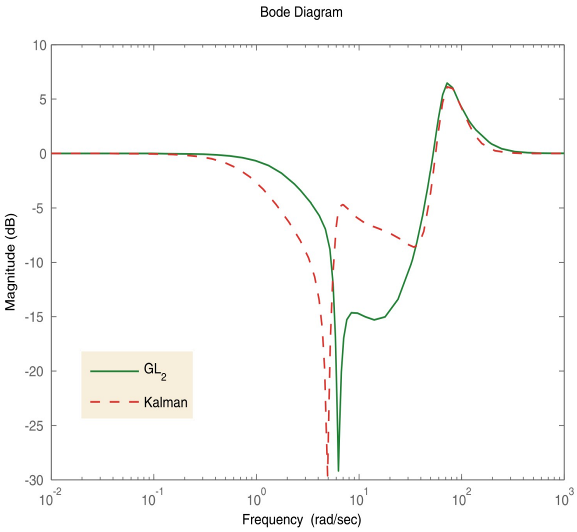

Fig. 3. Frequency response of the TF from disturbance estimation error to input disturbance'

4.2 *Bump response*

In the context of vehicle ride and handling, road disturbances are generally classified as shock and vibration (Hrovat, D. [1997], Chen, H. and Guo, K. [2005]). In the following, the performance of the designed estimators is assessed for the case of shock. Shocks are discrete events of relatively short duration and high intensity, for example, an isolated bump or pothole in an otherwise smooth road surface. Such a disturbance can be described as:

$$z_{rf}(t) = \begin{cases} \frac{A}{2}(1-\cos(\frac{2\pi V}{L}t)), & 0 \le t \le \frac{L}{V} \\ 0, & t > \frac{L}{V} \end{cases}$$

$$z_{rr}(t) = \begin{cases} \frac{A}{2}(1-\cos(\frac{2\pi V}{L}(t-\frac{l}{V}))), & \frac{l}{V} \le t \le \frac{L+l}{V} \\ 0, & \text{otherwise} \end{cases}$$

where A and L are the height and the length of the bump and $l = l_f + l_r$ is the length of the half-car. We choose $A = 0.06m$, $L = 5m$ and the vehicle forward velocity as $V = 20m/s (= 72Km/h)$. Figure 4 shows the estimation of the bump disturbance using both GL_2 and Kalman estimators. For comparison purposes the input bump itself is also shown in this figure. The results reveal that estimated bump using the GL_2 estimator coincides the input bump almost whole the time , whereas the Kalman estimator follows the input with some error, which is apparent in the plots.
It can be easily seen that the GL_2 estimator has almost the same performance level for all values of sprung mass, assuring stability and performance against mass variations and confirm the above expressions.

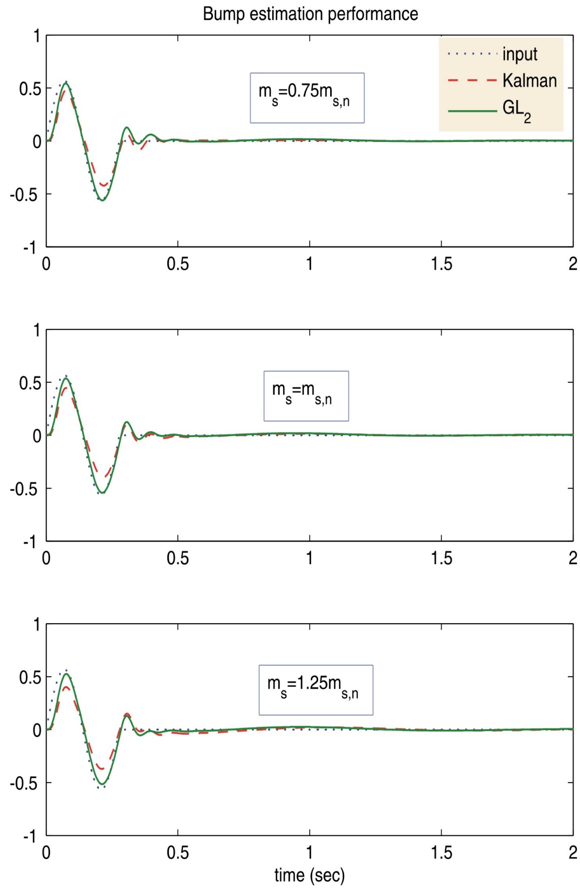

Fig. 4. Estimation of bump input

5. CONCLUSION

To estimate the disturbance applied to the steer wheel a GL_2 estimator was designed to deal with the system parametric uncertainties. Pole location constraints are also considered to care for the transient dynamics of the system. Moreover, the estimator suggested here, allows the designer to emphasize on specific states, within an specific frequency range, by appropriate selection of weighting functions. The designed estimator was compared with a Kalman one. The results showed that the designed GL_2 estimator has slightly better performance than the Kalman estimator for the nominal plant and unlike the Kalman estimator, maintains its performance over the entire range of uncertainty.

Employing this estimator in wheelbase preview control of active vehicle suspension will be some part the authors' future work.

Moreover, in the design procedure the correlation between front and rear wheel disturbances was ignored, which seems to lead to more improved performance of estimator. This will be considered in future works.

REFERENCES

D'andrea, R. Generalized L_2 synthesis. *IEEE Transactions on*

Automatic Control, 44:1145–1156, 1999.

Boyd, S., Ghaoui, L.E., Feron, E. and Balakishnan, V. *Linear Matrix Inequalities in system and control*. SIAM, Philadelphia, 1994.

Chen, H. and Guo, K. Constrained H_∞ control of active suspensions: an LMI approach. *IEEE Transactions on Control Systems Technology*, 13:412–421, 2005.

Chilali, M. and Pascal, G. H_∞ design with pole placement constraints: an LMI approach. *IEEE Transactions on Automatic Control*, 41 (3):358–367, 1996.

Foag, W. *Regelungstechnische Konzeption einer aktiven PKW-Federung mit 'Preview'*. Fortschritt-berichte VDI, 1990.

Gahinet, P., Nemirovski, A., Laub, A.J. and Chilali, M. *LMI control toolbox*. The Mathworks Inc., 1995.

Szaszi, I. Gaspar, P. and Bokor, J. Design of robust controllers for active vehicle suspension using the mixed μ synthesis . *Vehicle System Dynamics*, 40 (4):193–228, 2003.

Hac, A. Optimal linear preview control of active vehicle suspension. *Vehicle System Dynamics*, 21:167–195, 1992.

Hrovat, D. Survey of advanced suspension system developements and related optimal control applications. *Automatica*, 33:1781–1817, 1997.

Marzbanrad, J., Ahmadi, G., Zohoor, H. and Hojjat, Y. Stochastic optimal preview control of vehicle suspension. *Jounal of Sound and Vibration*, 275:973–990, 2004.

Scherer, C.W., Gahinet, P. and Chilali, M. Multi-objective output-feedback control via LMI optimization. *IEEE Transactions on Automatic Control*, 42:896–911, 1997.

Wang, J. and Wilson, D. A. Mixed $GL_2/H_2/GH_2$ control with pole placement and its application to vehicle suspension systems. *International Journal of Control*, 74(13):1353–1369, 2001.

Wu, L. and Chen, H.L. Complex stochastic wheelbase preview control and simulation of a semi-active motorcycle suspension based on hierarchical modeling method. *International journal of automotive technology*, 7(6):749–756, 2006.

Zhou, K., Doyle, J. and Glover, K. *Robust and Optimal Control*. Prentice Hall, 1996.